

XP-002143040

Spin-polarized Auger-electron spectroscopy

R. Allenspach,* D. Mauri,[†] M. Taborrelli, and M. Landolt

Laboratorium für Festkörperphysik, Eidgenössische Technische Hochschule, CH-8093 Zürich, Switzerland

(Received 30 October 1986)

A comprehensive review of spin-polarized Auger-electron spectroscopy on 3d transition-metal ferromagnets is presented. The kind of information obtained from the Auger-electron spin polarization depends on the particular transition involved. Decays with emission of a valence electron probe the local magnetization at the site where the transition occurs. Particularly, the super-Coster-Kronig $M_{23}M_{45}M_{45}$ transitions are well suited for monitoring magnetic behavior with elemental resolution. Details of the spectra are sensitive to screening and electron correlation effects as illustrated by a comparison between Fe and Ni. Furthermore, core-hole-only decays—as exemplified by the $L_{33}M_{23}M_{23}$ process—yield exchange-interaction strengths between partly filled shells on a single atom.

I. INTRODUCTION

Spin-polarized electrons are today widely used to probe two different aspects of solid-state physics: They reveal the symmetry properties of electronic wave functions in the case of nonmagnetic systems¹ and they reflect exchange interactions in magnetically ordered solids.^{2,3} Auger emission as a manifestation of a many-electron effect contains—in addition to its surface analytical power—invaluable information on correlation and screening. The combination of both spin polarization and Auger-electron spectroscopy is the natural extension of this standard technique. Essentially two distinct approaches are possible: The initial spin asymmetry in the process is either introduced by a magnetically ordered sample, or, alternatively, the incident electrons which create the core-hole excitation are spin polarized. So far, only the first approach has been realized,^{4,5} despite its limitation to magnetic systems, because of its evident simplicity.

In this paper, we present a comprehensive review of spin-polarized Auger-electron spectroscopy (SPAES) on 3d transition-metal ferromagnets. The aim is to show that SPAES is a technique for gaining element specific, as well as magnetic, information at one stroke. We point out what has been learned up to now from spin-polarization analysis in addition to the usual intensity measurements, and indicate what can be learned in principle if more refined theories are made available.

The paper is organized as follows: A short section is devoted to the description of the experimental setup. Then the essential concepts of SPAES are illustrated by means of the LMM Auger decays. Special interest is given to the core-hole-only $L_{33}M_{23}M_{23}$ transition where coupling between unfilled shells plays the key role. The $L_{33}M_{45}M_{45}$ line, on the other hand, involves two valence electrons and hence the problem of correlation is addressed. Later on, the MMM decays will serve to confirm the results found in the LMM transitions. We will show that we are able to distinguish two different excitation mechanisms for the creation of the initial hole in the

Auger process. Furthermore, many-electron effects above threshold have been identified thanks to their strong spin polarization. The paper finally concludes by comparing the two elements investigated, Fe and Ni, in particular, with respect to screening mechanisms of the initial core hole of the Auger process.

II. EXPERIMENTAL PROCEDURE

The experimental setup used in this work has been described previously in detail.⁶ To review, we present a schematic drawing in Fig. 1 and briefly mention a few essential points.

Unpolarized electrons of kinetic energy E_p between 80 and 2500 eV irradiate the sample, which is magnetized parallel to the surface. The angle of incidence θ is 70° off surface normal. The secondary electrons collected at normal emission (angular acceptance of $\pm 2.5^\circ$) are energy analyzed by means of a cylindrical-mirror analyzer with a resolution of $\Delta E/E = 1.1\%$. Subsequently, from the exit aperture of the analyzer the electrons are fed into a Mott detector for spin analysis.

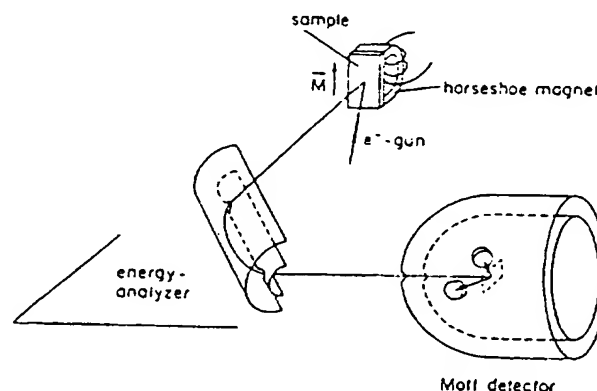


FIG. 1. Schematic experimental setup for measuring the spin polarization of Auger and secondary electrons.

Each polarization value is an average of two consecutive measurements with opposite sample magnetization to eliminate asymmetries due to the apparatus as well as to the spin-orbit coupling in the electron scattering process. Thus only the magnetic contribution to the polarization is retained.

Special attention has to be drawn to the magnetization of the sample. To guarantee constant magnetization over the large spot size of ≈ 1 mm, the sample has to be in a single-domain state. Its magnetic fringe fields, prohibitive in SPAES, are shortcut by a horseshoe-shaped magnet made from Armco iron. Good contact between the sample and the magnet is crucial. In the case of Fe the contact faces had to be mechanically polished to achieve a single-domain state of the crystal. The sample-magnet assembly is magnetized by applying a short current pulse through a coil wrapped around the magnet, and all measurements are taken in the remanent state.

The preparation of the single crystalline Fe and Ni surfaces followed standard procedures. The Fe crystal was annealed at ≈ 1100 K in 1 bar H_2 prior to insertion into the ultrahigh vacuum system (base pressure 4×10^{-10} Torr). Numerous cycles of Ne^+ sputtering at grazing incidence and subsequent annealing at ≈ 800 K established a sharp low-energy electron-diffraction pattern. All contaminants were below the detection limit of our Auger system. The measurements were performed slightly above room temperature ($T \approx 320$ K).

The Auger decays produce only small structures superimposed on the secondary electron cascade, both in the intensity and in the spin-polarization spectra. To obtain the net spin polarization of the Auger electrons from the measured data, we eliminate the secondary electrons created by cascade processes and the inelastically rediffused primary electrons by subtracting backgrounds both in the intensity I and the polarization P , using a power-law fit $I_0 = \alpha E^\beta + \gamma$ for the intensity⁷ and an assumed linear background for the spin polarization. The effective Auger spin polarization then is obtained as $P_{eff} = P_0 + (P - P_0)I/(I - I_0)$, where P_0 and I_0 are the respective backgrounds. This background subtraction introduces a relatively large uncertainty in our estimates of the net Auger polarizations, of the order of 20% of the estimated values. This of course is especially true for the low-energy MMM lines, because in their energy range both the intensity and polarization spectra vary strongly and therefore make a proper background subtraction difficult. The more qualitative conclusions we draw from these lines, however, do not depend on the subtleties of background subtraction.

III. LMM AUGER DECAYS IN 3d TRANSITION METALS

In the 3d transition metals the various decay channels of a 2p core hole give rise to intensity spectra which are of striking similarity for all elements. Two examples are depicted in Figs. 2 and 3, for single crystalline Fe and Ni, respectively. The only difference in the intensity spectra are the sharpening of the Auger structures involving valence electrons $L_3M_{23}M_{45}$ and $L_3M_{45}M_{45}$, in going

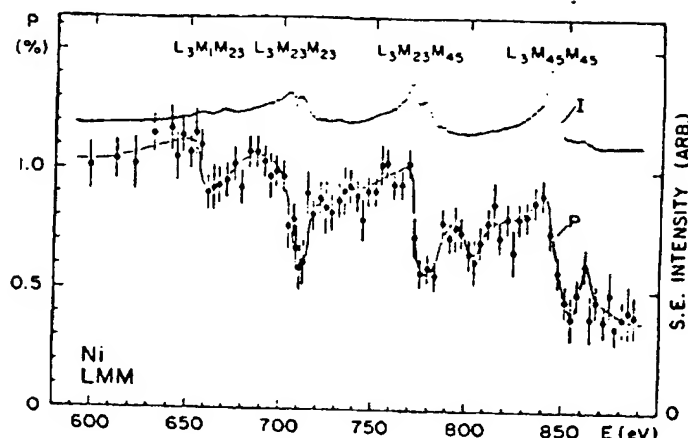


FIG. 2. Spin polarization P and intensity I vs kinetic energy of secondary electrons from Ni(100), excited with electrons of $E_p = 2100$ eV.

from Fe to Ni. This perfectly agrees with the general trend in the LMM spectra of 3d metals, which change from bandlike to more and more atomiclike if we proceed from Sc to Ge.⁸

The strong resemblance between Fe and Ni is apparently reflected in the polarization spectrum line shape as well. There is, however, a major difference between the two elements: The Ni spin polarization is much smaller than the one of Fe, the largest clearly resolved structures being of the order of less than 1%.

The effective polarizations of the LMM Auger transitions in Fe and Ni are calculated by the standard procedure of background subtraction (see Sec. II); they are summarized in Table I. The reliability is within 20% of the estimated values, and therefore the experimental uncertainty does not affect the semiquantitative discussion we will present below.

At first glance, we expect the effective spin polarization of the Auger lines to reflect the 3d band polarization,

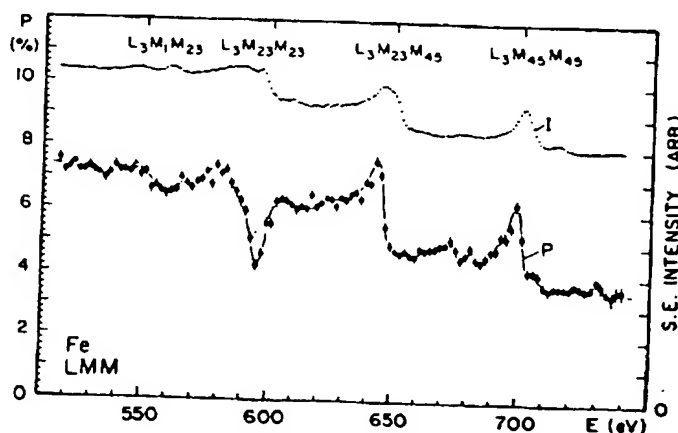


FIG. 3. Spin polarization P and intensity I vs kinetic energy of secondary electrons from Fe(100), excited with electrons of $E_p = 2500$ eV.

TABLE I. Effective Auger-spin polarizations (in %) of all prominent lines in Ni and Fe calculated as described in Sec. II. The errors are $\leq 20\%$ of the given values. Experimental band polarizations are taken from the spin polarization of secondary electrons at 30 eV, excited with primary energy of 2500 eV, the calculated values are derived from magnetic moments at $T=0$ K. For comparison, the values for $\text{Fe}_{13}\text{B}_{17}$ from Refs. 6 and 22 are also shown.

	Ni(100)	Fe(100)	$\text{Fe}_{13}\text{B}_{17}$
$L_{23}M_{23}M_{23}$ ($S=0$)	2	20	11
$L_{23}M_{23}M_{23}$ ($S=1$)	-1	-8	-15
$L_{23}M_{23}M_{45}$	3	27	16
$L_{23}M_{45}M_{45}$	3	27	19
$M_{23}M_{45}M_{45}$	10	37	22
$M_{11}M_{45}M_{45}$	2	40	
P_{ind} { expt.	4.3	26	12
{ calc.	5.7	27.5	21

since in any case the ferromagnetism in the 3d band induces the spin-polarization effects of the transition-metal Auger spectra. Obviously, there is a discrepancy between Ni and Fe. The LMM Auger lines in Ni are substantially less polarized than in Fe, even if we take the difference in band polarizations into account. We attribute this different behavior of Ni and Fe to a distinct mechanism which leads to the polarization of the Auger lines. We will see below that in Ni the polarization is determined by "resonant" $2p \rightarrow 3d$ excitation and subsequent Auger decay of the strongly polarized 2p hole, whereas in Fe the "normal" Auger process with an unpolarized 2p hole is polarized, too. For didactic purposes, we will first now discuss the somewhat special case of Ni, and then compare to the more typical (and unluckily more complicated) case of Fe.

A. Ni LMM transitions

Ni is a simple case because its ground state is (in the solid) a mixture of $3d^9$ and $3d^{10}$ configuration,⁹ with the 3d shell almost filled. The $3d^{10}$ configuration can be neglected in all the following arguments: An Auger process initiating at a closed shell (and hence nonmagnetic) atomic site is unpolarized. Our discussion thus concentrates on the $3d^9$ configuration. The creation of the initial hole in the Auger process starting from $3d^9$,

$$2p^6 3d^9 \rightarrow (2p^5 3d^9)_{\text{sc}} + eI,$$

leads to screening of the 2p hole. The weak polarization of the LMM lines suggests that this screening reduces the local band polarization considerably, i.e., screening is produced mainly by 3d electrons. We may assume

$$(2p^5 3d^9)_{\text{sc}} = 2p^5 3d^{10},$$

i.e., complete screening of the 2p hole by a local $3d^{10}$ configuration. This assumption is in accordance with the general opinion that screening within the 3d band is considerably more efficient than screening using a higher band. For perfect screening the normal LMM Auger process is unpolarized, because the full 3d shell has no net

spin moment.

This is essentially fulfilled for the Ni LMM Auger lines with their almost vanishing polarizations, see Fig. 2 and Table I. The small residual polarization is contributed by resonant Auger processes, which differ from the normal Auger process in the initial step:

$$2p^6 3d^9 \rightarrow (2p^5 3d^9)_{\text{sc}} + eI \quad (\text{normal}),$$

$$2p^6 3d^9 \rightarrow 2p^5 3d^{10} \quad (\text{resonant}).$$

In the resonant Auger process, the resonant excitation $2p \rightarrow 3d$ leads to a self-screened state with no additional screening charge necessary. The essential point is, that in Ni, in contrast to the normal excitation, the resonant $2p \rightarrow 3d$ excitation produces fully spin-down 2p holes since the available empty 3d states are of minority spin down only, and exchange processes with the primary electron are unimportant at the high-primary energy used in this study.¹⁰

For the fully polarized 2p holes in Ni, we can easily calculate the spin-polarization spectrum for the resonant Auger processes and compare it to the measured spectral behavior. Since the Auger decay starts from a $2p^5 3d^{10}$ configuration, the transition probabilities to the various two-hole final states^{11,12} may be approximated by the ones of Cu. The energetic position of the final-state terms are modified from the Cu values by substituting the 2p-, 3p-, and 3d-binding energies of Cu by the ones of Ni, taken from tabulated x-ray photoelectron spectroscopy (XPS) data.¹³ The spin polarization of all final states was calculated by Feldkamp and Davis:¹⁴ $P=1$ for singlets, and $P=-\frac{1}{3}$ for triplets. The combined effect of lifetime broadening and experimental resolution is taken into account by folding with a Lorentzian of FWHM of 7 eV. Without any adjustable parameter, we arrive at an overall spectral distribution which nicely fits the experiment; see Fig. 4.

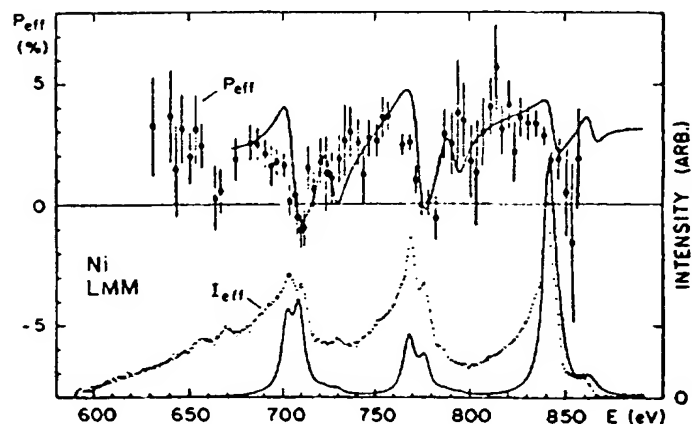


FIG. 4. Effective spin polarization P_{eff} and intensity I_{eff} of Ni(100) after background subtraction in the raw data of Fig. 2. The solid lines through the data points represent the calculation for the resonant processes as described in text; the polarization has been scaled by a factor $\frac{1}{10}$ to give reasonable agreement with the experimental data, and directly reveals the ratio of resonant to normal processes, R_{1p} .

From the ratio between measured and calculated effective polarizations, we determine the ratio between resonant and normal $2p$ -hole excitation at a primary electron kinetic energy of 2100 eV to be quite small, $R_{2p} \approx \frac{1}{30}$. With the assumption of complete screening of the $2p$ hole by a $3d^{10}$ configuration and a resulting resonant $2p \rightarrow 3d$ excitation strength of $\frac{1}{30}$ we arrive at a satisfactory description of the Ni *LMM* Auger spin polarizations. They must be compared now to the Ni *MMM* emission on one hand and to the Fe *LMM* transitions on the other. We postpone the rather lengthy discussion of Ni *MMM* and first compare them to the obviously very similar Fe *LMM* polarizations.

B. Fe *LMM* transitions

In Fe, the *LMM* Auger spectrum is much more difficult to interpret than in Ni. The Fe $3d$ shell with its $3d^6$ ground-state configuration is far from being filled, and moreover there are both empty $3d$ majority and minority spins above Fermi level. The Auger decays now start from an unfilled $3d$ shell with a nonzero spin even if screening effects are included. The complication then is that two unfilled shells must be incorporated in an atomic description of the Auger initial-state multiplets in the spirit of the so-called multiplet hole theory.¹⁵ But aside from these more technical difficulties we believe in a fundamental difference between Fe and Ni as far as the origin of the Auger spin polarization is concerned.

At first sight, the similarity between the Ni and Fe *LMM* spectra (see Figs. 2 and 3) seems to call for the same interpretation for the spin polarization in terms of resonant Auger processes. The marked contrast to Ni is, however, that the effective polarizations in Fe are large, see Table I. In fact, the effective polarizations in Fe are much too large to be explained by resonant Auger processes alone because of two reasons: First, the $2p \rightarrow 3d$ resonant excitation shows approximately the same strength as in Ni (at least within a factor of 2) as is concluded from energy-loss measurements. Second, the expected polarization for resonant excitation in Fe is smaller than in Ni since the empty $3d$ states are not exclusively spin down.

The major fraction of the large Auger polarization must therefore arise directly from normal Auger transitions. We thus neglect for a qualitative discussion the resonant excitations for the moment.

An explanatory description of the three prominent structures in the Fe *LMM* spectrum has already been given by Landolt and Mauri⁴ for Fe in the amorphous $\text{Fe}_{83}\text{B}_{17}$. The main difference between single-crystalline Fe and Fe in the metallic glass is, for the purposes of spin-polarized Auger spectroscopy, the strong magnetization reduction at the $\text{Fe}_{83}\text{B}_{17}$ surface within the probing depth of the experiment.⁶

The comparison of the effective polarizations scaled with the corresponding band polarizations in Table I then rather reveals the experimental uncertainty in background subtraction than fundamental physical differences. As a matter of fact, we do not expect a large influence of the missing long-range order in the metallic glass on such a

local process as an *LMM* Auger transition. Small broadening effects for amorphous Fe as observed by De Crescenzi *et al.*¹⁶ in energy-loss and Auger-electron derivative intensity studies are ascribed to changes in the valence band, but are too small to be observed with our experimental resolution of ≈ 5 eV at these energies.

Hence the interpretation of the polarization spectrum, can concentrate on either single-crystalline Fe or amorphous $\text{Fe}_{83}\text{B}_{17}$. A few remarks added to the earlier description seem to be appropriate, since new theoretical approaches have appeared.

Of particular interest is the strong polarization observed in the $L_3M_{23}M_{23}$ transition, where two holes in the $3p$ shell are left behind and no valence electron is directly involved in the Auger process. The intensity spectrum shows two peaks, corresponding to the singlet and triplet states of the $3p$ -hole pair. We observe negative effective polarization for the triplet and positive for the singlet state. Without calculating anything, we conclude from the nonvanishing polarization that the coupling of the involved shells to the ferromagnetic $3d$ band causes the polarization. The additional information gained by a polarization measurement allows to directly determine the exchange integrals between the partly filled shells.

Bennemann¹⁷ first tried to give a reasonable description based on a multiplicity argument. Kotani and Mizuta¹⁸ then presented a model calculation for Fe where the d -band ferromagnetism is described with a molecular field acting on localized spins $S^{3d}=1$, and where they introduce the exchange interactions among the two $3p$ holes, between $3d$ and $3p$ spins, and between $3d$ and $2p$ spins. The molecular field is deduced from T_C , and the intra- $3p$ exchange is obtained from the observed singlet-triplet splitting. The remaining two coupling constants are determined by a best fit to the polarization spectra. Interestingly, it is found that the $3d$ - $2p$ coupling, which yields slightly polarized $2p$ holes, is essential to reproduce the data. A more refined approach by the same authors¹⁹ even took lifetime broadening of the initial hole into account. The still remaining discrepancy between theory and experiment is the overall shift of the polarization spectrum compared to the intensity spectrum of ≈ 4 eV.

An alternative approach comes from cluster calculations. A four atom Fe cluster is able to reproduce singlet and triplet polarizations reasonably.²⁰ The lack of calculated transition intensities and improper counting of possible triplet final states prevents a better agreement with the experiment up to now.

Both model calculations, however, illustrate how SPAES reveals magnetic interaction between spins of partly filled shells of an atom in a ferromagnet. The extension of these models to the other *LMM* lines involving valence electrons is not straightforward. The quasiatomic approach does not apply for band electrons, and the cluster calculation, although principally equipped for valence-band Auger transitions, too, cannot be used because it yields a wrong d -band density of states due to the too small cluster size.²¹ Therefore the spectral distribution of the polarization on the valence-band lines cannot be reproduced by Ref. 20 at present. The simple estimate with the self-convolution of the occupied $3d$ band density

of states²² still seems to give best accordance with the experimental polarization on the $L_{23}M_{45}M_{45}$ line. More about this point will be said below in the discussion of the MMM transitions.

IV. MMM AUGER DECAYS IN $3d$ TRANSITION METALS

The super-Coster-Kronig $M_{23}M_{45}M_{45}$ Auger emission is the strongest decay channel of an excited $3p$ hole. The final state with the two additional holes in the $3d$ band is identical to the one of the $L_{23}M_{45}M_{45}$ Auger transition. The spectrum of the emitted $3d$ electrons, in a naive picture, reflects the self-convolution of the occupied part of the $3d$ bands. Thus, in a magnetic material, one expects to observe a spin polarization which is related to the band polarization at the atom where the Auger transition occurs.

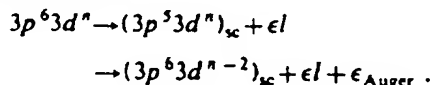
This crude approximation is appropriate both for the $L_{23}M_{45}M_{45}$ and the $M_{23}M_{45}M_{45}$ transition. Deviations from this picture due to many electron effects, however, should be visible at first in the MMM decay. The intensity and therefore the measured spin polarization is much larger on this low-energy line. The modifications to be expected will, if properly analyzed, contribute to the puzzle of screening and correlation.

Two points will have to be considered: First, the presence of the $3p$ hole leads to a rearrangement of the $3d$ and $4s,p$ orbitals at the site of the "impurity" in order to screen the positive charge. If screening is carried out by a $4s,p$ conduction electron, the modification of the $3d$ states is only minor and the magnetic moment remains unchanged. Screening by an extra $3d$ electron, however, will reduce the local magnetic moment. Second, the correlation among the two additional d holes left behind after an $M_{23}M_{45}M_{45}$ transition can be strong, and the two-hole excitation spectrum dominates over the one of the band-like extended hole states.^{8,11,23} The correlation shifts the Auger lines towards lower kinetic energies. We will discuss the differences between Fe and Ni mainly with regard to these points.

A. Fe MMM transitions

Figure 5 exhibits spin polarization and intensity spectra of the $M_{23}M_{45}M_{45}$ region in Fe(100). We attribute the wealth of features between 35 and 95 eV to Auger decays. The upper panel represents raw data, from which the effective Auger polarizations and intensities on the lower panel have been generated by background subtraction as described in Sec. II.

The main line in the intensity at 43 eV is the normal Auger process,



The corresponding P_{eff} spectrum shows a minimum near the high-energy end of the line. It is satisfactorily reproduced by a self-convolution of spin-split bands^{22,24} confirming that the valence-band Auger lines of Fe can be

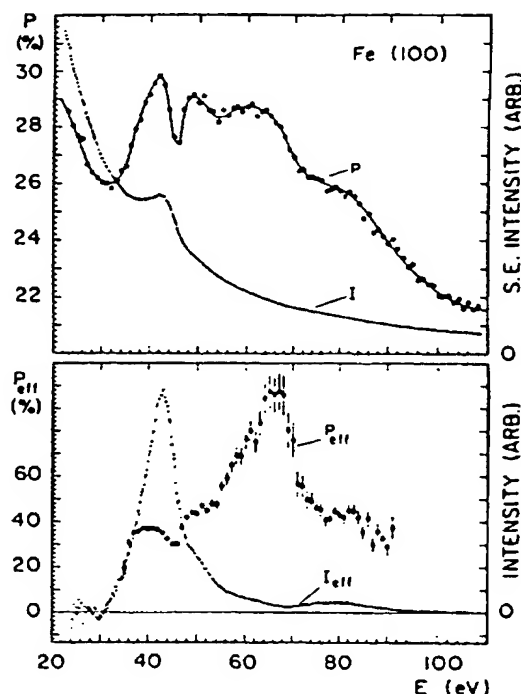
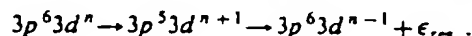


FIG. 5. Spin polarization P and intensity I vs kinetic energy of secondary electrons from Fe(100), excited with primary electrons of 2500 eV. Upper panel: raw data; lower panel: effective Auger electron signals after background subtraction.

described with a small effective correlation energy.¹¹ The effective spin polarization of this very intense MMM main line is large enough, $\approx 37\%$, to be used as a monitor for sign and magnitude of the element specific magnetization in composite magnetic systems, see Refs. 5 and 25.

Clearly above the $3p$ threshold, which is at 48 eV,¹³ a first gain satellite occurs at 51 eV. This satellite was observed in intensity spectra before and is interpreted as autoionization emission of a resonant $3p \rightarrow 3d$ excitation,²⁶



This interpretation is mainly based on three observations. First, in x-ray excited Auger spectra with photon energies far above the $3p \rightarrow 3d$ excitation energy, this satellite has not been identified. Second, the energetic position of this feature is clearly above the $3p$ threshold derived from XPS measurements. Moreover, the energy difference between the satellite and the Auger main line corresponds to the difference in energy-loss spectroscopy (ELS) and XPS energies for the whole $3d$ transition-metal series, reflecting the different final states left behind. Third, the intensity should be roughly proportional to the number of empty states available at Fermi level for the initial excitation $3p \rightarrow 3d$. In fact, we see a strong increase of the gain satellite intensity on oxidizing the Fe sample. This is expected because a partial charge transfer from Fe to O empties the $3d$ band. In contrast, however, if CO is adsorbed molecularly, no increase of the satellite is observed, again in line with the simple picture of band filling.

All these experiments seem convincing enough to interpret this gain satellite as autoionization or resonant Auger emission. The new information we contribute with Fig. 5 is that the resonant Auger emission in Fe is strongly polarized, $P_{\text{eff}} \approx 48\%$. A similar observation, less quantitative however, was reported for $\text{Fe}_{83}\text{B}_{17}$.⁴ This polarization is stronger than on the main line and indicates that the weak-correlation description is not appropriate for the resonant excitation process in Fe. If correlation was weak, we should be able to explain the polarization on the resonant line equally well by a self-convolution of the $3d$ density of states, modified compared with the main line by taking the partial polarization of the $3p$ hole into account. However, this correction does not change the calculated polarization appreciably,²² even with realistic energy bands.²⁴ We suggest therefore that inclusion of correlation is of vital importance to reproduce the data. A first approach would be a pure atomic description in terms of multiplets.¹⁴ This will neglect bandlike features but instead might be able to qualitatively explain the strong polarization.

The influence of oxidation on autoionization and Auger emission has recently been investigated by Ramsey and Russel^{27,28} in derivative intensity spectra. They see a shift of the Auger main line intensity to lower energy (≈ 4 eV) and no energy change but a strong intensity increase for the resonant channel. We see these alterations in the non-derivative intensity, too. In addition the overall spin polarization decreases on oxidation²⁵ because of reduced magnetic moments. Furthermore, we find that the effective polarizations on the $M_{23}M_{45}M_{45}$ main line and on the resonant feature are equal, $P_{\text{eff}} \approx 6\%$ for saturation coverage of oxygen. This observation of a relative reduction of the resonant Auger polarization compared to the normal one is supporting the interpretation of Ramsey and Russel.²⁷ They tentatively ascribe the resonant excitation in the Fe oxide to a $3p \rightarrow 4s, p$ transition rather than to a $3p \rightarrow 3d$ as in clean Fe. The expectation then is that the $3p$ hole in the oxide is almost unpolarized and hence the polarization is reduced.

The polarization maximum at 64 eV in Fig. 5, with a weak bump in intensity, is a newly discovered gain satellite in Fe. A similar feature has been observed in Ni. Its almost full spin polarization is restrictive for possible explanations. A possible process is for example an $M_{23}M_{45}N$ Auger decay of a resonant $3p \rightarrow 3d$ excitation accompanied by a monopole transition²⁹ of the kind $3d \rightarrow 4d$. This shake-up excitation is needed to supply the extra energy of ≈ 13 eV compared to the usual resonant process. Furthermore the decay must end up in a singlet state to emit fully spin-up polarized electrons.

An alternative explanation for the observed spin polarization above the $3p$ threshold is proposed by Nesbet:³⁰ The secondary electrons of the background undergo inelastic scattering, in particular $3p \rightarrow 3d$ losses. These were found to be strongly spin dependent near threshold¹⁰ leading to positive spin polarization because of strong exchange scattering. Nesbet suggests that the spin-polarization enhancement above the $3p$ threshold in Fe as well as in Ni is accounted for by $3p \rightarrow 3d$ energy losses of the background secondary electrons. The intensity, how-

ever, of these losses right at threshold is far too weak and therefore is not likely to be sufficient to cause the strong polarization enhancement.

The broad peak at the high-energy end of Fig. 5 is the $M_{145}M_{45}M_{45}$ Auger line of Fe centered around 82 eV. The observed polarization reasonably well corresponds to the one of the $M_{23}M_{45}M_{45}$ main line which has the same final state.

B. Ni MMM transitions

In Ni the situation is considerably different. There the resonantly and nonresonantly excited $3p$ hole states are degenerate: In resonant photoemission one finds that the MMM Auger emission and the d -band satellite occur at the same kinetic energy if the photon energy corresponds to the $3p \rightarrow 3d$ excitation energy.³¹ Therefore we assume that the screening of a $3p$ hole induces a local $3d^{10}$ configuration, i.e., $(3p^5 3d^9)_{\text{sc}} = 3p^5 3d^{10}$ in Ni, to obtain the identical excited state as for the resonant process.

Starting from a $3d^{10}$ configuration, the normal Auger emission away from resonance is expected to be unpolarized. In contrast to this expectation, an effective polarization $P_{\text{eff}} \approx 10\%$ on the Auger main line is found, see Fig. 6. The polarization arises from the resonant process, starting with a $3p \rightarrow 3d$ excitation. The $3p$ holes created are fully spin-down polarized, since only minority d holes exist in ferromagnetic Ni and the exchange scattering amplitude is weak at the high-primary electron energy used in the experiment.¹⁰ The correlation among the d holes now is important. In contrast to Fe, the effective Coulomb interaction U_{eff} in Ni is of the same magnitude as twice the bandwidth,¹¹ and hence atomic features dominate the d -band Auger spectra as in Cu or Zn. In close analogy to the LMM Auger lines, we can readily reproduce the spectral distribution of the effective polarization up to the $3p$ threshold of 62 eV,¹³ if we again take calculated Auger intensities³² and energetic positions¹¹ of the multiplets, and their spin polarization according to Ref. 14.

From the absolute value of P_{eff} one obtains the ratio of resonant $3p \rightarrow 3d$ to nonresonant $3p$ -hole excitations to be $R_{3p} \approx \frac{1}{5}$. This value is much larger than the corresponding one found for $2p$ -hole excitations, $R_{2p} \approx \frac{1}{20}$, at the same primary energy. This is not astounding at all, since it just reflects the fact that the oscillator strength of the $3p \rightarrow 3d$ transition is much larger than the $2p \rightarrow 3d$ transition because wave functions having the same principal quantum number are overlapping considerably.

A certain successful cross check for these values (and, implicitly, for our model of complete screening with a d electron) is provided by independent measurement of energy-loss intensity spectra. The consistency could be tested by some simple considerations, outlined briefly in the following. Neglecting interference effects described by Fano's formalism,³³ the peak-to-peak heights of the $2p \rightarrow 3d$ and $3p \rightarrow 3d$ electron energy loss, H_{2p} and H_{3p} , respectively, give a value for the strength of the resonant Auger decay. Comparing H to the number of all corresponding Auger decays (resonant plus normal), which is proportional to the area under the Auger lines, then esti-

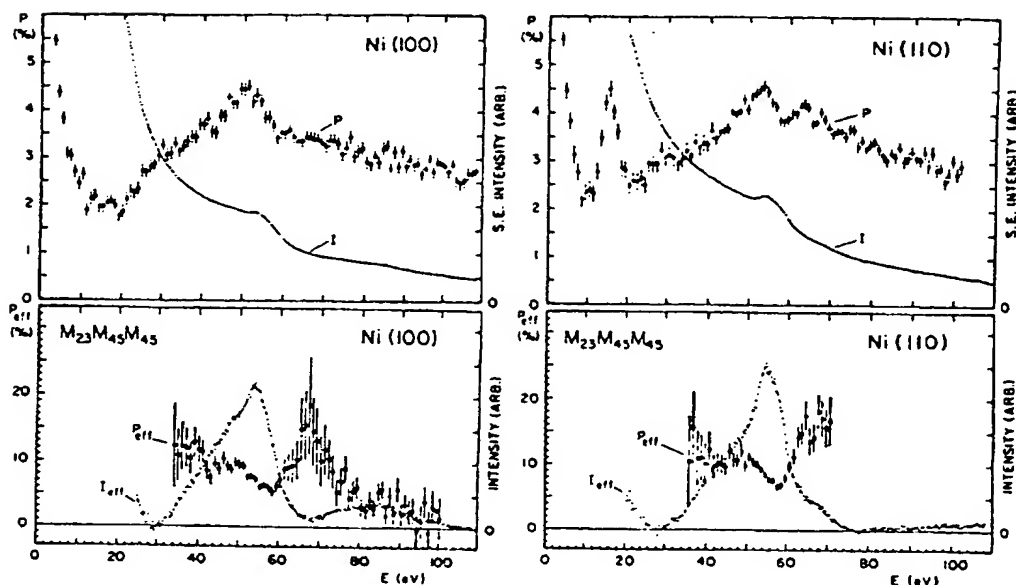


FIG. 6. Spin polarization P and intensity I vs kinetic energy of secondary electrons from Ni(100) and Ni(110), excited with primary electrons of 600 eV. Upper panels: raw data; lower panels: effective Auger signals after background subtraction.

mates the ratio of resonant to total Auger decays, which is approximately equal to resonant to normal decays. The result shows that $R_{3p}/R_{2p} \approx 4$ to 5, in agreement with the value estimated from comparison of measured and calculated spin-polarization spectra.

The determination of R_{3p} and R_{2p} in Ni is admittedly still very inaccurate in this first study. Nevertheless it shows that the distinction between normal and resonant Auger process even is accessible to the experiment if they are energetically degenerate, due to the power of spin analysis. In principle, these ratios may depend on the primary energy E_p of the electron initiating the Auger process. If E_p approaches threshold, both processes are known to die out, but the ratio of resonant to normal Auger process may change. Therefore the effective spin polarization on the $M_{23}M_{45}M_{45}$ Auger line in Ni can vary with E_p . We only checked that in the limited range of E_p between 200 and 2500 eV and did not find any E_p dependence. This is not a contradiction, however, because large effects can typically be expected only at energies in the near-threshold region, say $E_p \leq 100$ eV. A primary energy dependence of the Auger polarization has indeed been observed in Gd for the resonant $N_{45}N_{67}N_{67}$ transition.³⁴

The pronounced peak in P_{eff} at 66 eV lies above the $3p$ threshold energy of 62 eV. At present this structure is thought to be identical to the strongly spin-polarized upper gain satellite in Fe, namely an $M_{23}M_{45}N$ decay of a resonant $3p \rightarrow 3d$ excitation accompanied by a $3d \rightarrow 4d$ shake-up process. The Auger initial state is then, as in Fe, a highly excited $3p$ hole state, whereas the final state is the two hole "ground" state like the one on the Auger main line. This highly excited $3p$ hole with an excess energy of ≈ 13 eV has been found earlier in related methods like ELS,³⁵ XPS,³⁶ or x-ray absorption spectroscopy

(XAS).³⁷ Many interpretations have been given, but a consistent picture is still missing, even though new information has been added by SPAES. The high effective spin polarization leads to the conclusion that a singlet final state must predominate, again in striking similarity to Fe.

The intensity structures at 68 eV in Ni(110) and at 84 eV in Ni(100), respectively, are not related to Auger structures. They remain clearly visible for low-primary energies and even are enhanced for very low E_p of ≤ 90 eV, in contrast to what is expected for Auger related features. We ascribe them to critical points in the unoccupied band structure of Ni, which immediately explains the face dependence of the spectrum. Unfortunately, all calculated band structures end well below these energies. Other face-dependent features, like the highly polarized peak at ≈ 16 eV in the Ni(110) spectrum of Fig. 6, have been discussed in Ref. 38.

V. SCREENING OF THE INITIAL HOLE: CONCLUSIONS

In conclusion we state that the spin polarization of the MMM main lines in both cases, Fe and Ni, reflect the local band polarization, in completely different ways, however. The differences stem, at last, from a difference in the screening mechanism of the initial hole. In Ni, we have shown that all SPAES—as well as ELS measurements can be consistently explained by assuming total screening of the initial $3p$ (or $2p$) hole by an extra $3d$ electron. In all other $3d$ transition metals, on the other hand, the difference between XPS and ELS energies show that screening leads to a state quite distinct from resonant $3p$ (or $2p$) $\rightarrow 3d$ excitation. We assume therefore that this screening charge is supplied rather by $4s, p$ -band electrons

in Fe. A certain support for this idea comes from calculations of partial density of states. Kanamori³⁹ noted that in Ni in contrast to the other 3d transition metals the 4s,p density of states has a dip near Fermi energy. This makes screening by a 4s,p electron in Ni highly unlikely.

A serious test of our model, that screening in Ni leads to a local 3d¹⁰ configuration, would be an x-ray-excited spin-polarized Auger study. Tuning the photon energy through the 3p → 3d resonance should drastically change the polarization at the Auger-electron kinetic energy: The large polarization at resonance, where polarized holes are created, is expected to vanish for photon energies above resonance, and hence only largely unpolarized normal Auger processes are possible. This is a complementary experiment to the one performed by the Jülich group.⁴⁰ Whereas they were interested in the photon energy dependence of the resonant process and therefore investigated the constant initial state spectrum, we are concerned in the normal Auger process and hence in the constant final state.

In this paper, we discussed the more fundamental aspects of spin polarization for Auger-electron spectroscopy. Different single-crystalline faces of Fe and Ni have been investigated as model systems to understand the physics behind the measured spin polarization. We have seen that

quite distinct mechanisms lead to the highly-structured spin-polarization spectra. Core-hole-only transitions reflect exchange couplings between partly filled shells; normal and resonant Auger processes reveal different excitations, correlation, and screening, and transitions involving valence electrons directly monitor the local magnetization through the band polarization.

From the point of view of application, the availability of local magnetization is the greatest promise. The real power of SPAES is revealed in composite systems, where element specific sublattice magnetizations can be recorded. This topic has not been covered here. First studies in this direction have been performed recently.^{5,25} For a quantitative understanding of these fascinating applications, a thorough discussion of the mechanisms of SPAES is essential, and this is for what this paper is intended.

ACKNOWLEDGMENTS

We would like to thank P. Müller for assistance in the Ni measurements, and H. C. Siegmann for stimulating discussions. We are grateful to K. Brunner for expert and skillful technical support. This work has been sponsored in part by the Schweizerischer Nationalfonds and the Nationaler Energieforschungsfonds.

*Present address: IBM Zurich Research Laboratory, CH-8803 Rüschlikon, Switzerland.

†Present address: IBM Almaden Research Laboratory, San Jose, California 95120.

¹For a review, see F. Meier and D. Pescia, in *Optical Orientation*, edited by F. Meier and B. Zakharchenya (North-Holland, Amsterdam, 1984), p. 295.

²E. Kisker, K. Schröder, M. Campagna, and W. Gudat, *Phys. Rev. Lett.* **52**, 2285 (1984).

³J. Kirschner, *Phys. Rev. Lett.* **55**, 973 (1985).

⁴M. Landolt and D. Mauri, *Phys. Rev. Lett.* **49**, 1783 (1982).

⁵M. Taborelli, R. Allenspach, G. Boffa, and M. Landolt, *Phys. Rev. Lett.* **56**, 2869 (1986).

⁶D. Mauri, R. Allenspach, and M. Landolt, *J. Appl. Phys.* **58**, 906 (1985).

⁷E. N. Sickafus, *Phys. Rev. B* **16**, 1436 (1977).

⁸For a review, see J. C. Fuggle, in *Electron Spectroscopy*, edited by C. R. Brundle and A. D. Baker (Academic, London, 1981), Vol. 4.

⁹T. H. Upton and W. A. Goddard III, *Phys. Rev. Lett.* **42**, 472 (1979).

¹⁰D. Mauri, R. Allenspach, and M. Landolt, *Phys. Rev. Lett.* **52**, 152 (1984).

¹¹E. Antonides, E. J. Janse, and G. A. Sawatzky, *Phys. Rev. B* **15**, 1669 (1977).

¹²The L_2/L_3 intensity ratio in Ni was arbitrarily taken as $\frac{1}{2}$ of the calculated Cu values in order to account for the enhanced probability for $L_2L_3M_{45}$ decays in Ni, see Ref. 11.

¹³J. C. Fuggle and N. Mårtensson, *J. Electron Spectrosc. Relat. Phenom.* **21**, 275 (1980).

¹⁴L. A. Feldkamp and L. C. Davis, *Phys. Rev. Lett.* **43**, 151

(1979).

¹⁵C. S. Fadley, D. A. Shirley, A. J. Freeman, P. S. Bagus, and J. V. Mallow, *Phys. Rev. Lett.* **23**, 1397 (1969); C. S. Fadley and D. A. Shirley, *Phys. Rev. B* **2**, 1109 (1970).

¹⁶M. De Crescenzi, E. Colavita, L. Papagno, G. Chiarello, R. Scarmozzino, L. S. Caputi, and R. Rosei, *J. Phys. F* **13**, 895 (1983).

¹⁷K. H. Bennemann, *Phys. Rev. B* **28**, 5304 (1983).

¹⁸A. Kotani and H. Mizuta, *Solid State Commun.* **51**, 727 (1984).

¹⁹H. Mizuta and A. Kotani, *J. Phys. Soc. Jpn.* **54**, 4452 (1985).

²⁰M. M. Donovan, R. C. O'Handley and K. H. Johnson, *Proceedings of the 11th International Colloquium on Magnetic Films and Surfaces*, Asilomar, 1985 (unpublished); M. M. Donovan (private communication).

²¹D. R. Jennison, *J. Vac. Sci. Technol.* **20**, 548 (1982).

²²D. Mauri, Ph.D. thesis, Eidgenössische Technische Hochschule Zürich, 1983 (unpublished).

²³G. Tréglia, M. C. Desjonquères, F. Ducastelle, and D. Spanjaard, *J. Phys. C* **14**, 4347 (1981).

²⁴K. Schröder, E. Kisker, and A. Bringer, *Solid State Commun.* **55**, 377 (1985).

²⁵R. Allenspach, M. Taborelli, and M. Landolt, *Phys. Rev. Lett.* **55**, 2599 (1985).

²⁶S. D. Bader, G. Zajak, and J. Zak, *Phys. Rev. Lett.* **50**, 1211 (1983); G. Zajak, J. Zak, and S. D. Bader, *ibid.* **50**, 1713 (1983); G. Zajak, S. D. Bader, A. J. Arko, and J. Zak, *Phys. Rev. B* **29**, 5491 (1984).

²⁷M. G. Ramsey and G. J. Russel, *Phys. Rev. B* **30**, 6960 (1984).

²⁸M. G. Ramsey and G. J. Russel, *Phys. Rev. B* **32**, 3654 (1985).

²⁹T. A. Carlson, M. O. Krause, and W. E. Moddeman, *J. Phys.*

- (Paris) Colloq. 32, C4-76 (1971).
- ³⁰R. K. Nesbet, Phys. Rev. B 32, 390 (1985).
- ³¹C. Guillot, Y. Ballu, J. Paigné, J. Lecante, K. P. Jain, P. Thiry, R. Pinchaux, Y. Pétroff, and L. M. Falicov, Phys. Rev. Lett. 39, 1632 (1977).
- ³²E. J. McGuire, Phys. Rev. A 16, 2365 (1977).
- ³³U. Fano, Phys. Rev. 124, 1866 (1961).
- ³⁴M. Taborrelli, R. Allenspach, and M. Landolt, Phys. Rev. B 34, 6112 (1986).
- ³⁵R. E. Dietz, E. G. McRae, and J. H. Weaver, Phys. Rev. B 21, 2229 (1980); A. E. Meixner, R. E. Dietz, G. S. Brown, and P. M. Platzmann, Solid State Commun. 27, 1255 (1978); T. Jach and C. J. Powell, *ibid.* 40, 967 (1981).
- ³⁶S. Hüfner and G. K. Wertheim, Phys. Lett. 51A, 299 (1975).
- ³⁷F. C. Brown, C. Gähwiller, and A. B. Kunz, Solid State Commun. 9, 487 (1971).
- ³⁸E. Tamura and R. Feder, Phys. Rev. Lett. 57, 759 (1986).
- ³⁹J. Kanamori, in *Electron Correlations and Magnetism in Narrow-Band Systems*, edited by T. Moriya (Springer, Berlin, 1981), p. 102.
- ⁴⁰R. Clauberg, W. Gudat, E. Kisker, E. Kuhlmann, and G. M. Rothberg, Phys. Rev. Lett. 47, 1314 (1981).

THIS PAGE BLANK (USPTO)